
MCGAN: ENHANCING GAN TRAINING WITH REGRESSION-BASED GENERATOR LOSS

Baoren Xiao

Mathematics Department
University of College London
London
baoren.xiao.18@ucl.ac.uk

Hao Ni

Mathematics Department
University of College London
London
h.ni@ucl.ac.uk

Weixin Yang

Mathematical Institute
University of Oxford
Oxford
weixin.yang@maths.ox.ac.uk

ABSTRACT

Generative adversarial networks (GANs) have emerged as a powerful tool for generating high-fidelity data. However, the main bottleneck of existing approaches is the lack of supervision on the generator training, which often results in undamped oscillation and unsatisfactory performance. To address this issue, we propose an algorithm called Monte Carlo GAN (MCGAN). This approach, utilizing an innovative generative loss function, termed the regression loss, reformulates the generator training as a regression task and enables the generator training by minimizing the mean squared error between the discriminator’s output of real data and the expected discriminator of fake data. We demonstrate the desirable analytic properties of the regression loss, including discriminability and optimality, and show that our method requires a weaker condition on the discriminator for effective generator training. These properties justify the strength of this approach to improve the training stability while retaining the optimality of GAN by leveraging strong supervision of the regression loss. Numerical results on CIFAR-10 and CIFAR-100 datasets demonstrate that the proposed MCGAN significantly and consistently improves the existing state-of-the-art GAN models in terms of quality, accuracy, training stability, and learned latent space. Furthermore, the proposed algorithm exhibits great flexibility for integrating with a variety of backbone models to generate spatial images, temporal time-series, and spatio-temporal video data.

Keywords Generative adversarial networks · Image generation · Semi-supervised learning · Regression

1 Introduction

In recent years, Generative Adversarial Network (GAN) [1] has become one of the most powerful tools for realistic image synthesis. However, the instability of the GAN training and unsatisfying performance remains a challenge. To combat it, much effort has been put into developing regularization methods, see [2, 3, 4, 5]. Additionally, as [6] pointed out, the generator usually suffers gradient vanishing and instability due to the singularity of the denominator showed in the gradient when the discriminator becomes accurate. To address this issue, some work has been done to develop better adversarial loss [7, 8, 9]. As a variant of GAN, conditional GAN (cGAN) [10] is designed to learn the conditional distribution of target variable given conditioning information. It improves the GAN performance by incorporating conditional information to both the discriminator and generator, we hence have better control over the generated samples [11] [12] [13].

Unlike these works on the regularization method and adversarial loss, our work focuses on the generative loss function to enhance the performance of GAN training. In this paper, we propose a novel generative loss, termed as the regression loss \mathcal{L}_R , which reformulates the generator training as the least-square optimization task on real data. This regression loss underpins our proposed MC-GAN, an enhancement of existing GAN models achieved by replacing the original generative loss with our regression loss. This approach leverages the expected discriminator D^ϕ under the fake measure induced by the generator. Benefiting from the strong supervision lying in the regression loss, our approach enables the generator to learn the target distribution with a relatively weak discriminator in a more efficient and stable manner.

The main contributions of our paper are three folds:

- We propose the MCGAN methodology for enhancing both unconditional and conditional GAN training.
- We establish the theoretical foundation of the proposed regression loss, such as the discriminivity and optimality. Besides, we show the improved stability of the proposed MC-GAN. To illustrate, we provide a simple but clear example of Dirac-GAN, in which our proposed MCGAN successfully mitigate the issues of non-convergence of the conventional GANs by incorporating the regression loss.
- We empirically validate that MCGAN consistently enhances the performance of various GANs across various data, including image data, time series data, and video data. Our approach improves quality, accuracy, training stability, and learned latent space, showing its generality and flexibility.

Related work GANs have demonstrated their capacity to simulate high-fidelity synthetic data, facilitating data sharing and augmentation. Extensive research has focused on designing GAN models for various data types, including images [14], time series [15, 16, 17], and videos [18]. Recently, Conditional GANs (cGANs) have gained significant attention for their ability to generate synthetic data by incorporating auxiliary information [15, 19, 20]. For the integer-valued conditioning variable, conditional GANs can be roughly divided into two groups depending on the way of incorporating the class information: *Classification-based* and *Projection-based* cGANs [12, 21, 13, 11, 10, 22]. For the case where conditioning variable is continuous, the training of conditioning GANs is more challenging. For example, conditional WGAN suffers the difficulty in estimating the conditional expected discriminator of real data due to the need for recalibration per every discriminator update [19]. Attempts are made to mitigate this issue, such as conditional SigWGAN [19], which is designed to tackle this issue for time series data.

2 Preliminary

2.1 Generative adversarial networks

Generative adversarial network (GAN) [1] aims to learn the target distribution from real data. To this goal, GAN plays a min-max game between two networks: *Generator* and *Discriminator*. Let \mathcal{X} denote the target space and \mathcal{Z} be the latent space. Then *Generator*, denoted by G is defined as a parameterised function G that maps latent noise $z \in \mathcal{Z}$ to the target data $x \in \mathcal{X}$, i.e. $G : \Theta \times \mathcal{Z} \rightarrow \mathcal{X}$. *Discriminator* denoted by D discriminates between the real data and fake data generated by the generator, it is defined as a parameterised function that maps the data into real space \mathbb{R} , i.e., $D : \phi \times \mathcal{X} \rightarrow \mathbb{R}$. The generator and discriminator are trained to solve the following min-max game [1]:

$$\min_{\theta} \max_{\phi} \mathbb{E}_{\mu} [\log(D^{\phi}(X))] + \mathbb{E}_{\nu_{\theta}} [\log(1 - D^{\phi}(X))] . \quad (1)$$

In Eqn. (1), the discriminator is trained to maximise the binary cross entropy (BCE) loss while the generator is trained to minimise the BCE such that the fake measure induced by generator ν_{θ} coincides with μ . Let μ and ν_{θ} denote the true measure and fake measure induced by G_{θ} .

For the convenience of discussion, we can rewrite the GAN training objective (1) in a more generic form as follows:

$$\begin{aligned} \max_{\phi} \mathcal{L}_D(\phi; \theta) &= \mathbb{E}_{\mu} [f_1(D^{\phi}(X))] + \mathbb{E}_{\nu_{\theta}} [f_2(D^{\phi}(X))] , \\ \min_{\theta} \mathcal{L}_G(\theta; \theta) &= \mathbb{E}_{\nu_{\theta}} [h(D^{\phi}(X))] , \end{aligned} \quad (2)$$

where f_1 , f_2 and h are real-valued functions that can be chosen based on the adversarial loss (or metric) being used. To retrieve the original min-max objective Eqn. (1), we can set $f_1(x) = \log(x)$ and $f_2(x) = -h(x) = \log(1 - x)$. Apart from non-saturating loss, extensive studies are concerned with how to measure the divergence or distance between μ and ν_{θ} as the improved GAN loss function, which are instrumental in stabilising the training and enhancing the generation performance. Examples include *Hinge loss*[7], *Wasserstein loss*[9], *Least squares loss* [8], *Energy-based loss* [23] among others. Many of them satisfy the general form of Eqn. (2).

Example 1 Here are two examples:

- Hinge loss : $f_1(w) = f_2(-w) = -\max(0, 1 - w)$, and $h(w) = -w$.
- Wasserstein distance : $f_1(w) = f_2(-w) = w$, and $h(w) = -w + c_{\mu}$, where $c_{\mu} := \mathbb{E}_{X \sim \mu}[D^{\phi}(X)]$.

The Wasserstein distance is linked with the mean discrepancy. More specifically, let $d_{\phi}(\mu, \nu)$ denote the mean discrepancy between any two distributions μ and ν associated with test function D^{ϕ} defined as $d_{\phi}(\mu, \nu) = \mathbb{E}_{X \sim \mu}[D^{\phi}(X)] - \mathbb{E}_{X \sim \nu}[D^{\phi}(X)]$. In this case, $\mathcal{L}_G(\theta; \phi)$ could be interpreted as $d_{\phi}(\mu, \nu_{\theta})$.

2.2 Conditional GANs

Conditional GAN (cGAN) is a conditional version of a generative adversarial network that can incorporate additional information, such as data labels or other types of auxiliary data into both the generator and discriminative loss [10].

The goal of conditional GAN is to learn the conditional distribution μ of the target data distribution $X \in \mathcal{X}$ (i.e., image) given the conditioning variable (i.e., image class label) $Y \in \mathcal{Y}$. More specifically, under the real measure μ , $X \times Y$ denote the random variable taking values in the space $\mathcal{X} \times \mathcal{Y}$. The marginal law of X and Y are denoted by P_X and P_Y , respectively.

The conditional generator $G_\theta : \mathcal{Y} \times \mathcal{Z} \rightarrow \mathcal{X}$ incorporates the additional conditioning variable to the noise input, and outputs the target variable in \mathcal{X} . Given the noise distribution Z , $G_\theta(y)$ induces the induced fake measure denoted by $\nu_\theta(y)$, which aims to approximate the conditional law of $\mu(y) := \mathbb{P}(X|Y = y)$ under real measure μ . The discriminator: $D^\phi : \mathcal{X} \rightarrow \mathbb{R}$. The task of training an optimal conditional generator is formulated as the following min-max game:

$$\mathcal{L}_D(\phi, \theta) = \mathbb{E}_{Y \sim P_Y} [\mathbb{E}_{\mu(Y)} [f_1(D^\phi(X))] + \mathbb{E}_{\nu_\theta(Y)} [f_2(D^\phi(X))]], \quad (3)$$

$$\mathcal{L}_G(\theta; \phi) = \mathbb{E}_{Y \sim P_Y} [\mathbb{E}_{X \sim \nu_\theta(Y)} [h(D^\phi(X))]], \quad (4)$$

where f_1 , f_2 and h are real value functions as before. Different from the unconditional case, \mathcal{L}_D and \mathcal{L}_G has in the outer expectation $\mathbb{E}_{y \sim P_Y}$ due to Y being a random variable.

3 Monte-Carlo GAN

3.1 Methodology

In this section, we propose the Monte-Carlo GAN (MCGAN) for both unconditional and conditional data generation. Without loss of generality, we describe our methodology in the setting of the conditional GAN task.¹

Consider the general conditional GAN model composed with the generator loss \mathcal{L}_G (Eqn. (4)) and the discrimination loss \mathcal{L}_D outlined in the last subsection. To further enhance the GAN model, we propose the following MCGAN by replacing the generative loss \mathcal{L}_G with the following novel regression loss for training the generator from the perspective of the regression, denoted by \mathcal{L}_R ,

$$\mathcal{L}_R(\theta; \phi) := \mathbb{E}_{(X,Y) \sim \mu} [|D^\phi(X) - \mathbb{E}_{x \sim \nu_\theta(Y)} [D^\phi(x)]|^2], \quad (5)$$

where the expectation is taken under the joint law μ of X and Y . We optimize the generator's parameters θ by minimizing the regression loss $\mathcal{L}_R(\theta; \phi)$. We keep the discriminator loss and conduct the remaining min-max training as before.

The name for Monte Carlo in MCGAN is due to the usage of the Monte Carlo estimator of expected discriminator output under the fake measure. This innovative loss function reframes the conventional generator training into a mean-square optimization problem by computing the l^2 loss between real and expected fake discriminator outputs.

Next, we explain the intuition behind \mathcal{L}_G and its link with optimality of conditional expectation. Let us consider a slightly more general optimization problem for \mathcal{L}_R :

$$\min_{f \in \mathcal{C}(\mathcal{Y}, \mathbb{R})} \mathbb{E}_\mu [|D^\phi(X) - f(Y)|^2], \quad (6)$$

It is well known that the conditional expectation is the optimal l^2 estimator. Therefore, the **unique minimizer** to Eqn (6) is given by the conditional expectation function $f^* : \mathcal{Y} \rightarrow \mathbb{R}$, defined as

$$f^*(y) = \mathbb{E}_\mu [D^\phi(X) | Y = y].$$

This fact motivates us to consider the conditional expectation under the fake measure, $\mathbb{E}_{\nu_\theta(Y)} [D^\phi(X)]$, as the model for the mean equation f^* . It leads to our regression loss \mathcal{L}_R , where we replace f by $\mathbb{E}_{\nu_\theta(Y)} [D^\phi(X)]$ in Eqn. (6).

Minimising the regression loss \mathcal{L}_G would enforce the conditional expectation of $D^\phi(X)$ under fake measure $\nu_\theta(Y)$ to approach that under the conditional true distribution $\mu(Y) = \mathbb{P}(X|Y)$ for any given D^ϕ . Suppose that $(G_\theta)_{\theta \in \Theta}$ provides a rich enough family of distributions containing the real distribution μ . Then there exists $\theta^* \in \Theta$, which is a minimizer of $\mathcal{L}_R(\theta, \phi)$ for all possible discriminator's parameter ϕ , and it satisfies that

$$\mathbb{E}_{\mu(Y)} [D^\phi(X)] = \mathbb{E}_{\nu_{\theta^*}(Y)} [D^\phi(X)]. \quad (7)$$

¹The unconditional GAN can be viewed as the conditioning variable is set to be the empty set.

It implies that no matter whether the discriminator D^ϕ achieves the equilibrium of GAN training, the regression loss \mathcal{L}_R is a valid loss to optimize the generator to match its expectation of D^ϕ between true and fake measure.

Moreover, we highlight that our proposed regression loss can effectively mitigate the challenge of the conditional Wasserstein GAN (c-WGAN). To compute the generative loss of c-WGAN, one needs to estimate the conditional expectation $\mathbb{E}_{\mu(Y)}[D^\phi(X)]$. However, when the conditioning variable is continuous, estimating this conditional expectation becomes computationally expensive or even infeasible due to the need for recalibration with each discriminator update. In contrast, our regression loss does not need the estimator for $\mathbb{E}_{\mu(Y)}[D^\phi(X)]$.

3.2 Comparison between \mathcal{L}_R and \mathcal{L}_G

In this subsection, we delve into the training algorithm of the regression loss \mathcal{L}_R and illustrate its advantages of enhancing the training stability in comparison with the generator loss \mathcal{L}_G . For ease of notation, we consider the unconditional case. To optimize the generator's parameters θ in our MCGAN, we apply gradient-descent-based algorithms and the updating rule of θ_n is given by

$$\begin{aligned}\theta_{n+1} &= \theta_n - \lambda \frac{\partial \mathcal{L}_R}{\partial \theta} \Big|_{\theta=\theta_n} \\ &= \theta_n - 2\lambda \underbrace{(\mathbb{E}_\mu[D^\phi(X)] - \mathbb{E}_{\nu_{\theta_n}}[D^\phi(X)])}_{d_\phi(\mu, \nu_{\theta_n})} H(\theta_n, \phi),\end{aligned}\tag{8}$$

where λ is the learning rate and

$$H(\theta, \phi) = \mathbb{E}_{z \sim p(z)} [\nabla_\theta G^\theta(z)^T \cdot \nabla_x D^\phi(G^\theta(z))].\tag{9}$$

Note the gradient $\frac{\partial \mathcal{L}_R}{\partial \theta}$ takes into account not only $\nabla_x D^\phi(x)$ but also $d(\mu, \nu_\theta)$ - the discrepancy between the expected discriminator outputs under two measures μ and ν_θ .

In contrast, employing the generator loss \mathcal{L}_G , the generator parameter θ is updated by the following formula:

$$\begin{aligned}\theta_{n+1} &= \theta_n \\ &- \lambda \mathbb{E}_{z \sim p(z)} [h'(D^\phi(G^{\theta_n}(z))) \nabla_\theta G^{\theta_n}(z)^T \Big|_{\theta=\theta_n} \cdot \nabla_x D^\phi(G^{\theta_n}(z))].\end{aligned}\tag{10}$$

One can see that Eqn. (10) depends on the discriminator gradients $\nabla_x D^\phi(G^{\theta_n}(z))$ heavily.

MCGAN benefits from the strong supervision of \mathcal{L}_R , which provides more control over the gradient behaviour during the training. When θ is close to the optimal θ^* , even if D^ϕ is away from the optimal discriminator, $d_\phi(\mu, \nu_\theta)$ would be small and hence leads to stabilize the generator training. However, it may not be the case for the generator loss as shown in Eq. (10), resulting in the instability of generator training. For example, this issue is evident for the Hinge loss where $h(x) = x$ as shown in [3].

3.3 Illustrative Dirac-GAN example

To illustrate the advantages of MCGAN, we present a toy example from [3], demonstrating its resolution of the training instability in Dirac-GAN. The Dirac-GAN example involves a true data distribution that is a Dirac distribution concentrated at 0. Besides, the Dirac-GAN model consists of a generator with a fake distribution $\nu_\theta(x) = \delta(x - \theta)$ with $\delta(\cdot)$ is a Dirac function and a discriminator $D^\phi(x) = \phi x$.

We consider three different loss functions for both \mathcal{L}_D and \mathcal{L}_G : (1) *binary cross-entropy loss* (BCE), (2) *Non-saturating loss* and (3) *Hinge loss*, resulting GAN, NSGAN and HingeGAN, respectively. In this case, the unique equilibrium point of the above GAN training objectives is given by $\phi = \theta = 0$.

In this case, the updating scheme of training GAN is simplified to

$$\begin{cases} \phi_{n+1} = \phi_n + \lambda f'(-\phi_n \theta_n) \theta_n, \\ \theta_{n+1} = \theta_n - \lambda h'(\phi_n \theta_n) \phi_n. \end{cases}$$

where f is specified as $f(x) = -\log(1 + \exp(x))$. By applying MCGAN to enhance GAN training, the update rules for the MCGAN model parameters θ and ϕ are modified as follows:

$$\begin{cases} \phi_{n+1} = \phi_n + \lambda f'(\phi_n \theta_n) \theta_n, \\ \theta_{n+1} = \theta_n - \lambda 2(\phi_n \theta_n - \phi_n c) \phi_n. \end{cases}$$

Fig. 1 (a-c) demonstrates that GAN, NSGAN and Hinge GAN all fail to converge to obtain the optimal generator parameter $\theta^* = 0$. That is due to the fact that the updating scheme of θ depends heavily on the ϕ . When ϕ fails to converge to zero, θ keeps updating itself even if it has reached zero, and the non-zero θ further encourages ϕ updating away from 0, which results in a vicious cycle and failure of both generator and discriminator. In contrast, Fig. 1(d) of MCGAN training demonstrates that the generator parameter θ successfully converges to the optimal value 0 thanks to the regression loss in (5) to bring the training stability of the generator.

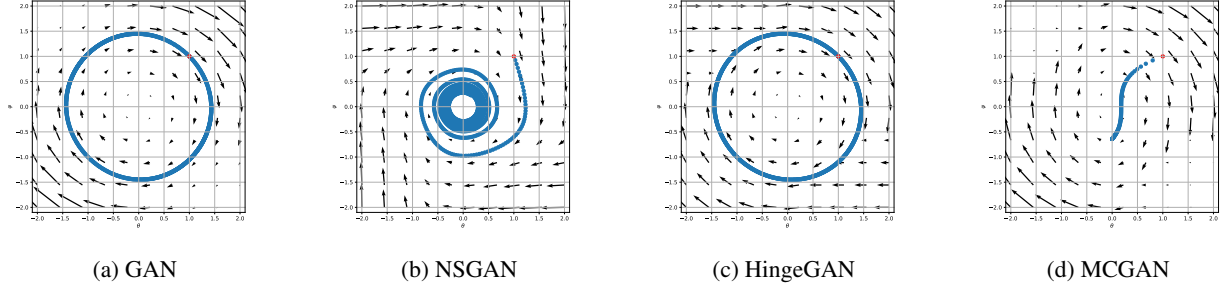


Figure 1: Dirac-GAN example

3.4 Discriminability and optimality of MCGAN

To ensure that MCGAN training leads to the optimal generator $\nu_{\theta^*} = \mu$, one needs the sufficient discriminative power of D^ϕ . The discriminative power of the discriminator is determined by the discriminative loss function \mathcal{L}_D . The discriminative loss function \mathcal{L}_D is usually defined as certain divergences, such as JS divergence in GAN [1], and computing such divergence involves finding the optimal discriminator that optimizes the objective function, which might be challenging in practice. See [24] for a comprehensive description of the discriminative loss function.

Instead of requiring an optimal discriminator, we introduce the weaker condition, the so-called *discriminability* of the discriminator D^ϕ to ensure the optimality of the generator for the MCGAN training.

Definition 1 (Discriminability) A discriminator

$$\begin{aligned} \mathcal{P}(\mathcal{X}) \times \mathcal{P}(\mathcal{X}) \times \mathcal{X} &\rightarrow \mathbb{R} \\ (\mu, \nu, x) &\mapsto D^{\phi_{\mu, \nu}}(x), \end{aligned} \quad (11)$$

where $\phi_{\cdot, \cdot} : \mathcal{P}(\mathcal{X}) \times \mathcal{P}(\mathcal{X}) \rightarrow \Phi$, is said to have discriminability if there exist two constants $a \in \{-1, 1\}$ and $c \in \mathbb{R}$ such that for any two measures $\mu, \nu \in \mathcal{P}(\mathcal{X})$, it satisfies that

$$a(D^{\phi_{\mu, \nu}}(x) - c)(p_\mu(x) - p_\nu(x)) > 0, \quad (12)$$

for all $x \in \mathcal{A}^{\mu, \nu} := \{x \in \mathcal{X} : p_\mu(x) \neq p_\nu(x)\}$. We denote the set of discriminators with discriminability as \mathcal{D}_{Dis} .

The discriminability of the discriminator can be interpreted as the ability to distinguish between ν and μ point-wisely over $\mathcal{A}^{\mu, \nu}$ by telling the sign (or the opposite sign) of $p_\mu(x) - p_\nu(x)$. In (12), if $a = 1$, the constant c can be regarded as a criterion in the sense that $D^{\phi_{\mu, \nu}}(x) - c$ is positive when $p_\mu(x) > p_\nu(x)$ and vice versa.

The discriminability covers a variety of optimal discriminators in GAN variants. We present in Table 1 a list of optimal discriminators of some commonly used GAN variants along with their values of a and c . The detailed description can be found in Appendix A.4.

Although discriminability can be obtained by training the discriminator via certain discriminative loss functions, it is worth emphasizing that the discriminator does not necessarily need to reach its optimum to obtain discriminability. In the case of BCE, the optimal discriminator is given by

$$D^{\hat{\phi}_{\mu, \nu \theta}^*}(x) = \frac{p_\mu(x)}{p_\mu(x) + p_{\nu \theta}(x)}. \quad (13)$$

However, we can find a non-optimal discriminator with discriminability as follows:

$$\hat{D}^{\phi_{\mu, \nu \theta}^*}(x) = D^{\phi_{\mu, \nu \theta}^*}(x) - \frac{1}{5} \left(D^{\phi_{\mu, \nu \theta}^*}(x) - \frac{1}{2} \right) \mathbf{1}_{\{p_\mu(x) > p_{\nu \theta}(x)\}} \quad (14)$$

Name	Discriminative loss	$D^*(x)$	a	c
Vanilla GAN	Binary cross-entropy	$\frac{p_\mu(x)}{p_\mu(x)+p_{\nu_\theta}(x)}$	1	1/2
LSGAN	Least square loss	$\frac{\alpha p_\mu(x)+\beta p_{\nu_\theta}(x)}{p_\mu(x)+p_{\nu_\theta}(x)}$	$\text{sign}(\alpha - \beta)$	$\frac{\alpha+\beta}{2}$
Geometric GAN	Hinge loss	$2\mathbb{1}_{\{p_\mu(x)\geq p_{\nu_\theta}(x)\}} - 1$	1	0
Energy-based GAN	Energy-based loss	$m\mathbb{1}_{\{p_\mu(x)<p_{\nu_\theta}(x)\}}$	$\text{sign}(-m)$	$\frac{m}{2}$
f -GAN	VLB on f -divergence	$f'\left(\frac{p_\mu(x)}{p_{\nu_\theta}(x)}\right)$	1	$f'(1)$

Table 1: List of common discriminative loss functions that satisfy strict discriminability

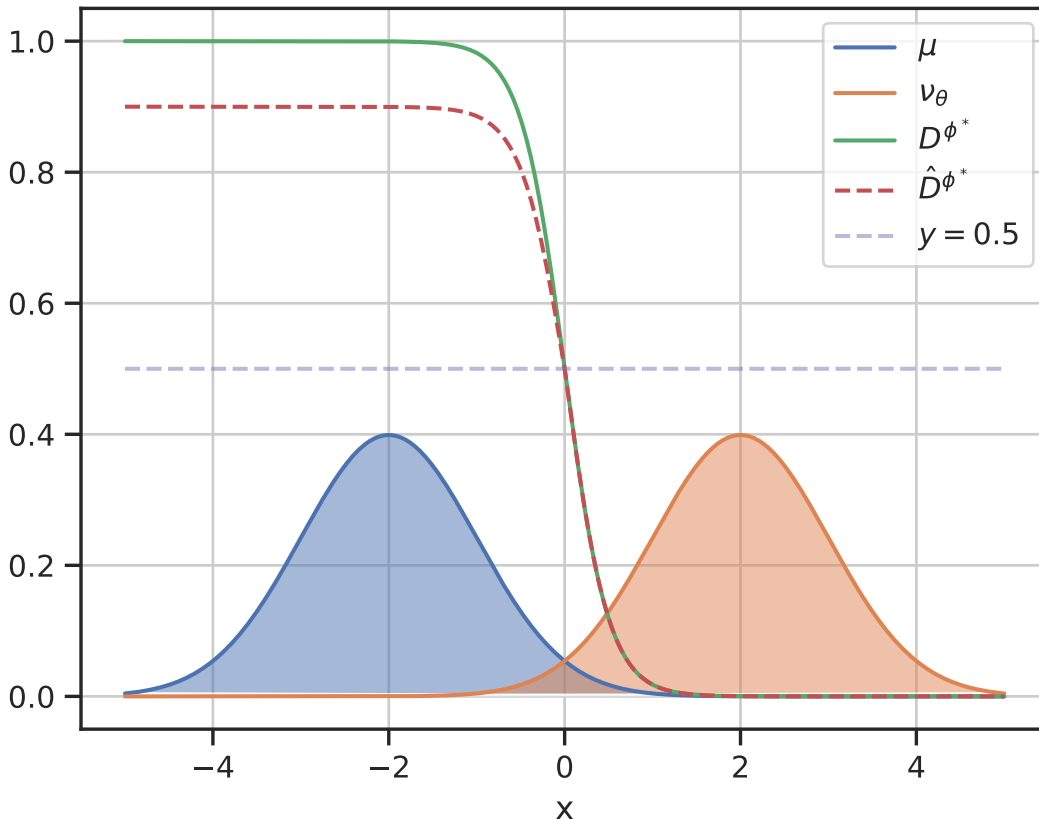


Figure 2: One illustration on the discriminability of the discriminator. In this example, $\mu \sim \mathcal{N}(-2, 1)$, $\nu_\theta \sim \mathcal{N}(2, 1)$. The optimal discriminator is given by (2) and the weaker version of discriminator \hat{D}^{ϕ^*} is defined in Eqn. (13).

It is easy to verify that $(D^{\hat{\phi}^*, \nu_\theta}(x) - 1/2)(p_\mu(x) - p_{\nu_\theta}(x)) > 0$, and $D^{\hat{\phi}^*, \nu_\theta}(x) \in (0, 1)$ for all $x \in \mathcal{X}$ as permitted by the feasible set. Hence, it has discriminability, although it is not optimal. We also present a 1-D example in Figure 2.

Now we establish the optimality of $\mu = \nu_\theta$ in the following theorem under the regularity condition defined in Assumption 3.1.

Assumption 3.1 Let H be defined in Eqn. (9). The equality $H(\theta, \phi) = \vec{0}$ holds only if (θ, ϕ) reaches the equilibrium point where $\nu_\theta = \mu$.

This assumption is made because that $H(\theta, \phi) = \bar{0}$ outside the equilibrium point usually means the failure of the discriminator (say a constant function), which is of no interest to us. By making this assumption, we focus on the case where the discriminator is powerful enough to guide the generator training.

Theorem 3.1 *Assume Assumption 3.1 holds, and let $\phi'_{\cdot, \cdot} : \mathcal{P}(\mathcal{X}) \times \mathcal{P}(\mathcal{X}) \rightarrow \Phi$ be a parameterization map such that $D^{\phi'_{\cdot, \cdot}} : \mathcal{P}(\mathcal{X}) \times \mathcal{P}(\mathcal{X}) \times \mathcal{X} \rightarrow \mathbb{R}$ has discriminability, i.e. $D^{\phi'_{\cdot, \cdot}} \in \mathcal{D}_{Dis}$. If θ^* is a local minimizer of $\mathcal{L}_G(\theta; \phi'_{\mu, \nu_\theta}, \mu)$ defined in (5), then $\nu_{\theta^*} = \mu$.*

Theorem 3.1 demonstrates that to learn the data distribution μ , MCGAN do not restrict the discriminator to reach its optimum; the discriminability is sufficient, which is again attributed to the strong supervision provided by regression loss \mathcal{L}_R .

4 Properties of MCGAN

4.1 Relation to f -divergence

Given the optimal discriminator (2), the vanilla GAN objective (1) can be interpreted as minimizing *Jensen-Shannon divergence* between μ and ν_θ , subtracting a constant term $\log(4)$. The generator is therefore trained to minimize the Jensen-Shannon divergence. Similarly, [8] also showed that optimizing LSGANs yields minimizing the Pearson χ^2 divergence between real and fake measures.

Given (13), we are also able to explore the connection between MCGAN and f -divergence. As proven in Lemma 4.1, when considering the optimal discriminator (13), the difference between real and fake expected discriminator output in (8) can be interpreted as an f -divergence between μ and $\bar{\nu}$, where $\bar{\nu} := \frac{(\mu + \nu)}{2}$ represents the averaged measure with density $p_{\bar{\nu}}(x) := \frac{p_\mu(x) + p_{\nu_\theta}(x)}{2}$.

Lemma 4.1 *Given the optimal discriminator in (13), optimizing the MCGAN objective (5) is equivalent to minimizing the square of f -divergence:*

$$\nabla_\theta \mathcal{L}_G(\theta; \phi^*) = \nabla_\theta [\text{Div}_f(\mu | \bar{\nu})]^2, \quad (15)$$

where $f(x) = x(x - 1)$.

Lemma 4.1 establishes a connection between MCGAN and f -divergence, illustrating the information-theoretic aspects of the MCGAN framework. Unlike the $\text{KL}(\nu | \mu)$ induced in non-saturating loss [6], this $\text{Div}_f(\mu | \bar{\nu})$ can avoid mode dropping by assigning moderate cost on the occasions where $p_\mu(x) \gg p_{\nu_\theta}(x)$.

4.2 Improved stability

Lack of stability is a well-known issue in GAN training, and it arises due to several factors. Arjovsky et al. [6] provides insights into this instability issue of non-saturating loss. The instability is analysed by modelling the inaccurate discriminator as an optimal discriminator perturbed by a centred Gaussian process. Given this noisy version of the optimal discriminator, it can be shown that the gradient of non-saturating loss follows a centred Cauchy distribution with infinite mean and variance, which leads to massive and unpredictable updates of the generator parameter. Hence it can be regarded as the source of training instability.

In contrast, we prove that the proposed regression loss function in MCGAN can overcome the instability issue. Moreover, we relax the condition of the noise vector from the independent Gaussian distribution to a more general distribution.

Theorem 4.1 *Let $D^{\phi_\epsilon}(x)$ be a noisy version of optimal discriminator such that $D^{\phi_\epsilon}(x) = D^{\phi^*}(x) + \epsilon_1(x)$ and $\nabla_x D^{\phi_\epsilon}(x) = \nabla_x D^{\phi^*}(x) + \epsilon_2(x)$ for $\forall x \in \mathcal{X}$, where $\epsilon_1(x)$ and $\epsilon_2(x)$ are two uncorrelated and centred random noises that are indexed by x and have finite variance.² Then for $\mathcal{L}_G(\theta; \phi)$ in (5), we have*

$$\mathbb{E}[\nabla_\theta \mathcal{L}_G(\theta; \phi_\epsilon)] = \nabla_\theta \mathcal{L}_G(\theta; \phi^*), \quad (16)$$

and the variance of $\nabla_\theta \mathcal{L}_G(\theta; \phi_\epsilon)$ is finite and depends on the difference between μ and ν_θ . Specifically, when $\nu_{\theta^*} = \mu$, we have $\nabla_\theta \mathcal{L}_G(\theta^*; \phi_\epsilon) = 0$ almost surely.

²This assumption of centred random noise is made due to the fact that as the approximation gets better, this error looks more and more like centred random noise due to the finite precision [6].

Theorem 4.1 implies that given an inaccurate discriminator, the expected value of the gradient of $\mathcal{L}_G(\theta; \phi)$ in (5) is the accurate gradient given by the optimal discriminator and its variance is finite. More importantly, its variance is determined by the discrepancy between μ and ν_θ , specifically when the fake measure produces the real measure, the gradient is zero almost surely, indicating improved training stability.

4.3 Relation to feature matching

In order to enhance the generative performance, a feature matching approach is proposed in [25] which adds to the generative loss function an additional cost that matches the statistic of the real and generated samples given by the activation on an intermediate layer of the discriminator. The generator hence is trained to generate fake samples that reflect the statistics (features maps) of real data rather than just maximizing its discriminator outputs.

To be specific, suppose we have a feature map ψ that maps each $x \in \mathcal{X}$ to a feature vector $\psi(x) = (\psi_1(x), \psi_2(x), \dots, \psi_n(x)) \in \mathbb{R}^n$ where each $\psi_i \in C_b(\mathcal{X})$, then the feature matching approach adds to the generative loss function an additional cost defined as:

$$R_{\text{fm}}(\theta; \phi) = \|\mathbb{E}_\mu[\psi(x)] - \mathbb{E}_{\nu_\theta}[\psi(x)]\|_2^2. \quad (17)$$

Although empirical results indicate that feature matching is effective, it lacks a theoretical guarantee that minimizing the difference of features can help us reach the Nash equilibrium or optimality $\nu_\theta = \mu$. Hence (17) is commonly used as a regularization term rather than an individual loss function like the one proposed in our MCGAN.

In the case of MCGAN, if we construct the discriminator as a linear transformation of the feature map, i.e. $D^\phi = \phi^T(\psi(x), \mathbf{1})$ where $\phi \in \mathbb{R}^{n+1}$ is a linear functional. Given the novel generative loss function in (5), we have

$$\nabla_\theta \mathcal{L}_G(\theta; \phi) = \nabla_\theta \|\mathbb{E}_\mu[\phi^T(\psi(x), \mathbf{1})] - \mathbb{E}_{\nu_\theta}[\phi^T(\psi(x), \mathbf{1})]\|^2.$$

Here, the generator is also trained to match the feature maps of real samples and fake samples, but in a weighted average way. By using the linear transformation on the feature map, the discriminator is trained to focus on the most relevant features and assign them larger weights while assigning relatively smaller weights to less important features. As a result, the generator is trained to match the feature maps more efficiently.

5 Numerical experiments

To validate the effectiveness of the proposed MCGAN method, we conduct extensive experiments on a variety of generation tasks on image, time-series, and video data. We mainly focus on the images for in-depth analysis in this section, and briefly introduce our attempts for the extensions to time-series and video data in the last two subsections.

The training algorithm of MCGAN for conditional generation task can be found in Algorithm 1 in Appendix C. We also put extra experimental details in Appendix B for reproducibility.

5.1 Datasets for image generation

We conduct conditional image generation tasks on the CIFAR-10 and CIFAR-100 datasets [26]. We conduct conditional image generation tasks on the CIFAR-10 and CIFAR-100 datasets [26]. CIFAR-10 is a widely used benchmark dataset in conditional image generation tasks. It consists of 60,000 32x32 RGB images for 10 different classes with 6,000 images each. The whole dataset is split into a training set of 50k images and a test set of 10k images if required for real distribution computing in some evaluation metrics. CIFAR-100 is similar to CIFAR-10 in terms of image size and dataset size but has 100 classes containing 600 images each.

5.2 Architectures, hyperparameters, and training techniques

5.2.1 Backbone GAN architectures

We employ BigGAN [27] and cStyleGAN2 [28] architectures as the backbones for image generation experiments.

BigGAN [27], as a member of projection-based cGAN, is a collection of recent best practices in conditional image generation, and it is widely used due to its satisfactory generation performance on high-fidelity image synthesis. We use the BigGAN architecture with the same regularization methods like *Exponential Moving Averages* (EMA) [29] and *Spectral Normalization* [4] have already been adopted. We adopt BigGAN’s PyTorch implementation³ and shows the architectural details in Table 5 for completeness.

³<https://github.com/PeterouZh/Omni-GAN-PyTorch>

cStyleGAN2 [30], is an improved and conditional version of the original StyleGAN, is a generative adversarial network (GAN) architecture designed for creating high-quality, diverse images. It addresses artifacts, enhances image quality, and has been widely used for generating realistic portraits and artwork. We adopt the code from the Github repository in [30]⁴. and use the default hyperparameter setting. The only difference is the minor modification we made to incorporate our MC method.

5.2.2 Loss functions

Since our MCGAN replaces the original generative loss in Eqn. (4) with the regression loss in Eqn. (5) and keeps the discriminator loss, we use two popular discriminator’s loss functions as baselines: the Hinge loss baseline and the BCE loss baseline.

5.2.3 Hyperparameters

For the CIFAR-10 experiment, the batch size is set to 32. We adopt the Adam optimizer in all experiments, with betas being 0.0 and 0.999. For both of the generator and discriminator, the learning rates are set to 0.0002 and the weight decay is 0.0001. The model is updated by using *Exponential Moving Average* starting after the first 5000 iterations. The generator is updated once every 3 times the discriminator is updated. For the CIFAR-100 experiment, we have fewer training samples for each class, so we update the discriminator 4 times per generator training as a more accurate discriminator is needed. Each experiment is conducted on one Quadro RTX 8000 GPU.

5.2.4 Training techniques

Leaky Clamp To stabilize the training of our regression loss, we employ the *Leaky Clamp* function to limit the discriminator output in a reasonable range so that the distance between fake and real discriminator output will not exceed a predetermined range. The leaky clamp function is defined as

$$C_{(lb,ub)}(x) = \begin{cases} lb + \alpha(x - lb) & \text{if } x \leq lb \\ x & \text{if } lb \leq x \leq ub \\ ub + \alpha(x - ub) & \text{if } ub < x \end{cases}$$

where $\alpha \in (0, 1)$ is a small slope for values outside the range $[lb, ub]$. Just similar to the negative slope in Leaky ReLU [31], the α in the Leaky Clamp function is used to prevent from vanishing gradient problem. And by applying this Leaky Clamp on the discriminator output when computing the regression loss, we are able to mitigate the early collapse problem.

Data augmentation To alleviate the overfitting and improve the generalization on the small training set, especially for CIFAR-100 where each class has scarce samples, we increase data efficiency by using the *Differentiable Augmentation* (DiffAug) [30] which imposes various types of augmentations on real and fake samples [30, 32, 33]. We adopt *Translation + Cutout* policy as suggested in [30]. Besides, we also apply horizontal flips when loading the training dataset as in [13].

5.3 Evaluation metrics

To assess the quality of images generated, we employ three quality metrics *Inception Score* (IS), *Fréchet Inception Distance* (FID), and *Intra Fréchet Inception Distance* (IFID) together with two recognizability metrics *Weak Accuracy* (WA) and *Strong Accuracy* (SA).

Inception Score [25] (IS) is a popular metric to evaluate the variety and distinctness of the generated images. It is given by

$$IS = \exp\{\mathbb{E}_{X \sim \nu_\theta} [D_{KL}(P(Y|X)||P(Y))]\} \quad (18)$$

where D_{KL} is the KL-divergence between the conditional class distribution $P(Y|X)$ and marginal class distribution of the $P(Y) = \mathbb{E}[P(Y|X)]$. The conditional class distribution $P(Y|X)$ is computed by *InceptionV3* network pre-trained on ImageNet. The higher IS, the better the quality. By the definition, the IS does not consider real images, so cannot measure how well the fake measure induced by the generator is close to the real distribution. Other limitations, as noted in [34], are: high sensitivity to small changes in weights of the Inception network, and large variance of scores. To consider both diversity and realism, the following FID and IFID are employed as well.

⁴<https://github.com/mit-han-lab/data-efficient-gans/tree/master>

Fréchet Inception Distance [35] (FID) compares the distributions of Inception embeddings of real and generated images, denoted by p_d and p_θ respectively. Under the assumption that the features of images extracted by the function f are of multivariate normal distribution. The FID score of p_θ w.r.t p_d is defined as

$$\text{FID}(p_d, p_\theta) = \|\mu_r - \mu_g\|^2 + \text{Tr}(\Sigma_r + \Sigma_g - 2(\Sigma_r \Sigma_g)^{\frac{1}{2}}), \quad (19)$$

where (μ_r, Σ_r) and (μ_g, Σ_g) denote the mean and covariance matrix of the feature of real and generated image distribution respectively. Given a data-set of images $\{x_i\}_i^N$ and the Inception embedding function f , the Gaussian parameters (μ_r, Σ_r) are then approximated as

$$\mu = \frac{1}{N} \sum_{i=0}^N f(x_i), \quad \Sigma = \frac{1}{N-1} \sum_{i=0}^N (f(x^{(i)} - \mu))(f(x^{(i)} - \mu))^T.$$

We can see from (19) that FID directly compares the distribution of features of real and fake images. However, the Gaussian assumption made in FID computation might not be met in practice. Also, FID has high sensitivity to the sample size — a small size might cause over-estimation of the real FID.

Intra Fréchet Inception Distance [36] (IFID) is used to quantify intra-class diversity. It is defined as the average of conditional FID given every class $y \in \mathcal{Y}$, i.e.,

$$\text{FID}(p_d, p_\theta) = \frac{1}{|\mathcal{Y}|} \sum_{y \in \mathcal{Y}} \text{FID}(p_d(y), p_\theta(y)),$$

where

$$\begin{aligned} \text{FID}(p_d(y), p_\theta(y)) = \\ \|\mu_r(y) - \mu_g(y)\|^2 + \text{Tr}(\Sigma_r(y) + \Sigma_g(y) - 2(\Sigma_r(y)\Sigma_g(y))^{\frac{1}{2}}). \end{aligned}$$

The combination of IS, FID, and IFID provides a comprehensive evaluation for generated image quality assessment. IS and FID are measured between 50K generated images given 10 different random seeds in this paper, and IFID is the average intra-class results of FID.

Recognizability is as crucial as realism and diversity in a good image generative model, therefore two classification accuracy are adopted—a weak accuracy (WA) measured by a two-layer convolutional neural network⁵ and a strong accuracy (SA) by the ResNet-50 [37]. Both classifiers are pre-trained on the same training set as for the generative model. The WA discerns subtle differences for better inter-model comparison, while the SA is more accurate for intra-model latent space analysis.

5.4 Evaluations of conditional image generation on CIFAR-10

5.4.1 Learning curves in training

In Figure 3, we plot the learning curves in terms of FID and IS during the training. It shows that the MC method tends to have much faster convergence and ends at a considerably better level in both baselines of using Hinge loss and BCE loss.

5.4.2 Quantitative results

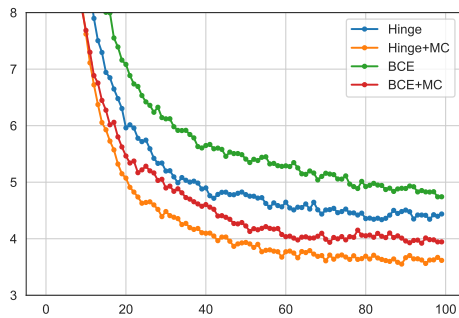
The quantitative results in Table 2 show that our MC method considerably improves all the baselines independently of different discriminative losses. Specifically, when using Hinge loss as the discriminative loss function along with DiffAug, the MC method can improve the FID from 4.43 to 3.61, which is comparable to most state-of-the-art models [5]. Also, its IS score also increased from 9.61 to 9.96, indicating better diversity of the generated samples.

For the recognizability metrics, we generated 10k (same setting as the test set) images using BigGAN backbone. The WA rates are 62.56%, 52.09%, and 54.71% for the real test set, the generated set from Hinge baseline, and the generated set from Hinge + MC, respectively. Our MC method’s images perform closer to the real test set than the baseline’s images, showing better distribution matching to the real data in terms of recognizability. The SA rate of our MC method is 83.42% compared to 93.65% of the real test set, showing that we generate fairly recognizable fake images.

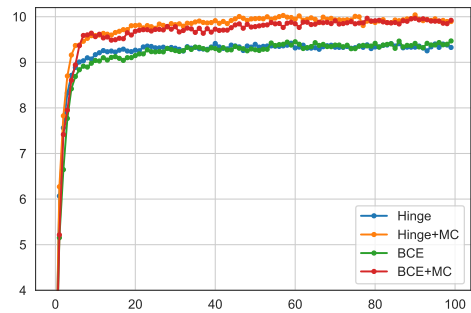
5.4.3 Qualitative results

The qualitative results are shown in Figure 4 with only a small amount of images (in red boxes) misclassified by our classifier.

⁵https://pytorch.org/tutorials/beginner/blitz/cifar10_tutorial.html



(a) FID ↓



(b) IS ↑

Figure 3: The learning curves in terms of (a) Fréchet Inception Distance and (b) Inception Score along the training on the CIFAR-10 dataset using BigGAN with different loss combinations.

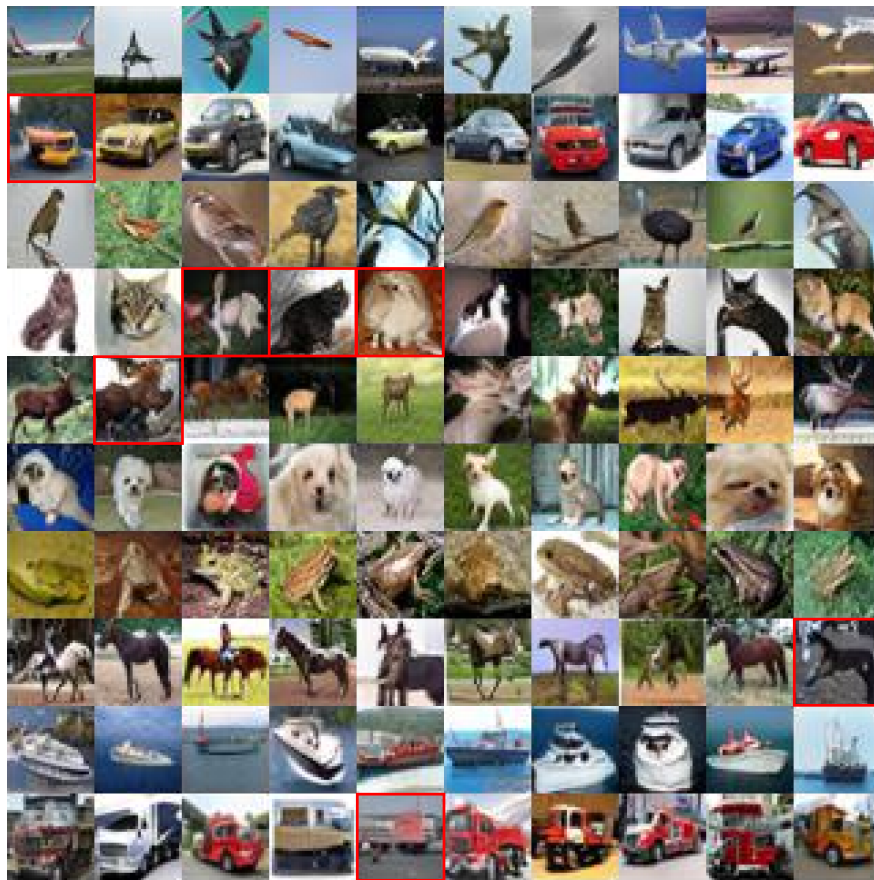


Figure 4: CIFAR-10 samples generated by the BigGAN backbone trained via Hinge + DiffAug + MC. Images in each row belong to one of the 10 classes. Images misclassified by ResNet-50 are in red boxes.

Loss	Hinge				BCE		
Metrics	IS \uparrow	FID \downarrow	IFID \downarrow		IS \uparrow	FID \downarrow	IFID \downarrow
Original	9.27 ± 0.11	5.31	16.20		9.301 ± 0.14	5.55	16.62
+DiffAug	9.61 ± 0.06	4.43	14.60		9.51 ± 0.11	4.71	14.83
+MC	9.66 ± 0.09	4.51	14.71		9.62 ± 0.09	4.61	14.82
+MC+DiffAug	9.96 ± 0.12	3.61	13.60		9.94 ± 0.10	3.93	13.72

Table 2: Quantitative results of image generation on CIFAR-10 using BigGAN w/o and with our MC method and Differentiable Augmentation.

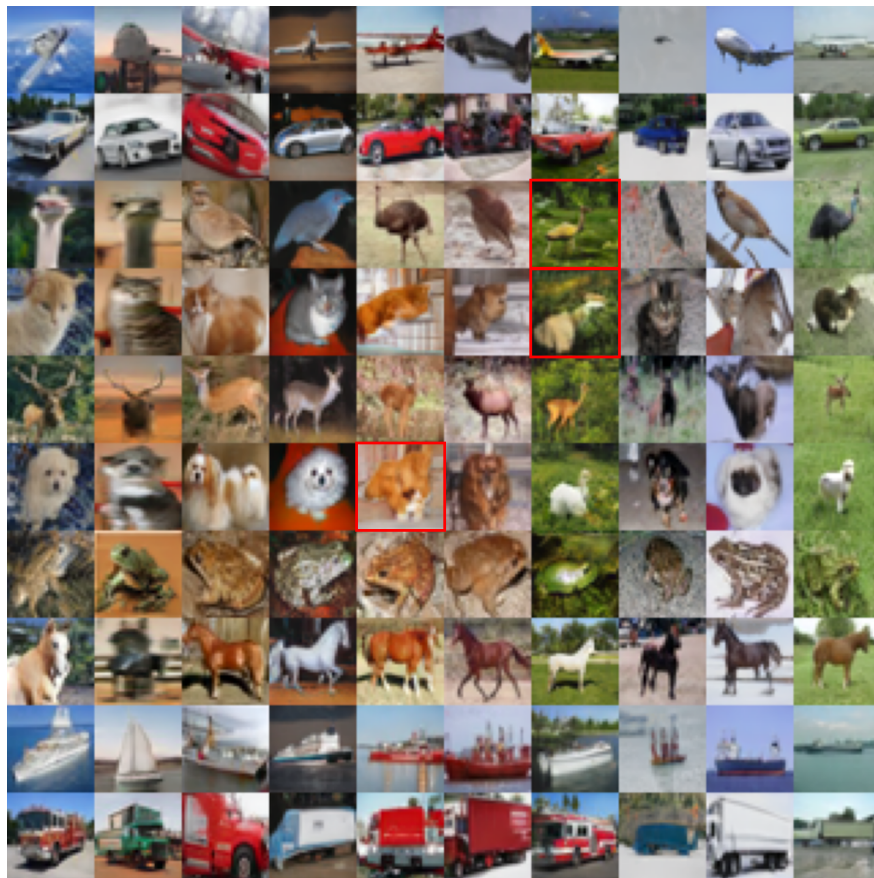


Figure 5: CIFAR-10 samples generated by the cStyleGAN2 backbone trained via Hinge + DiffAug + MC. Images in each row belong to one of the 10 classes. Images misclassified by ResNet-50 are in red boxes.

5.4.4 Results based on cStyleGAN2 backbone

In addition, we use cStyleGAN2 as the backbone for evaluation, summarize the results in Table 3, and show the qualitative results in Figure 5. We can see from Table 3 that under both Hinge and BCE losses, the proposed MC method is able to improve their FID by around 0.08. Among them, Hinge + MC + DiffAug achieves the best FID 2.16, outperforming most of the algorithms using StyleGAN2 as the backbone [13, 5, 38].

Based on our best model using cStyleGAN2, we plot the FID of each class in Figure 6. It shows that among all classes, the MC method consistently outperforms its counterparts. Cats and dogs are the two classes where all models have their worst FID. The proposed MC method is able to improve the FID of these two classes by around 0.45, which is a considerable gap.

Loss	Hinge				BCE		
Metrics	IS \uparrow	FID \downarrow	IFID \downarrow		IS \uparrow	FID \downarrow	IFID \downarrow
+DiffAug	10.1859	2.2475	11.4037		10.1281	2.4387	11.6191
+MC+DiffAug	10.2608	2.1650	11.0351		10.0995	2.3595	11.3004

Table 3: Quantitative results of image generation on CIFAR-10 using cStyleGAN2 w/o and with our MC method and Differentiable Augmentation.

Loss	Hinge				BCE		
Metrics	IS \uparrow	FID \downarrow	IFID \downarrow		IS \uparrow	FID \downarrow	IFID \downarrow
Original	10.73 \pm 0.10	8.31	83.36		10.81 \pm 0.14	8.37	81.89
+DiffAug	10.72 \pm 0.13	7.37	80.00		10.71 \pm 0.08	7.61	80.48
+MC	11.39 \pm 0.10	6.97	80.20		11.59 \pm 0.12	6.99	80.91
+MC+DiffAug	11.81\pm 0.06	5.77	76.26		11.90\pm 0.08	5.85	77.33

Table 4: Quantitative results of image generation on CIFAR-100 using BigGAN w/o and with our MC method and Differentiable Augmentation.

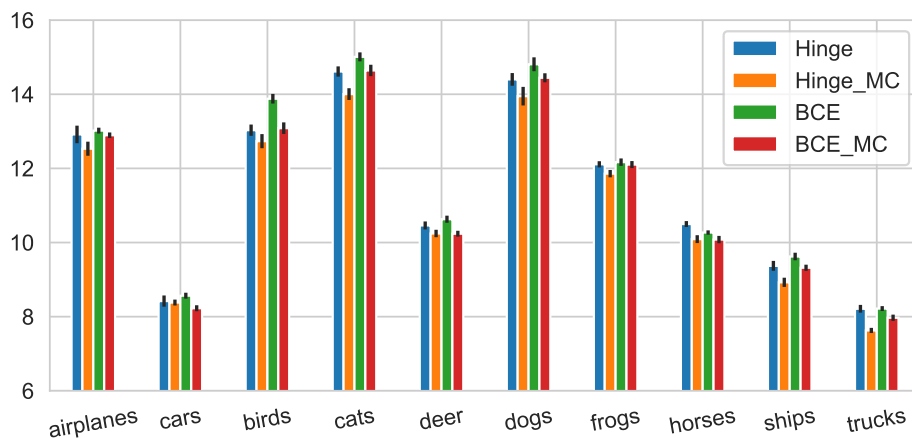


Figure 6: FID \downarrow of each class on CIFAR-10 dataset.

5.4.5 Evaluation of training stability

In Figure 7, we also plot the training dynamics of models trained on CIFAR-10 dataset. It is clear that the FID dynamic of the model trained with MC method is more stable than that of the original Hinge GAN and converged to a better level. In Figure 7b and 7c, the dynamics of $\mathbb{E}\|\nabla_x D^\phi(x)\|_2^2$ and $\text{Var}\|\nabla_x D^\phi(x)\|_2^2$ also indicates that the discriminator gradient $\nabla_x D^\phi$ of Hinge+MC is less volatile, which can result in better training stability of its generator due to its reliance on the sensitivity of $\nabla_x D^\phi$.

5.4.6 Latent space analysis

The latent space learned by the generator is expected to be continuous and smooth so that small perturbations on the conditional input can lead to smooth and meaningful modifications on the generated output. To explore the latent space, we interpolate between each pair of randomly generated images by linearly interpolating their conditional inputs. The results are shown in Figure 8. Intermediary images between a pair of images from two different classes are shown in each row with their confidence score distributions below. The labels of the two classes are shown on the left and

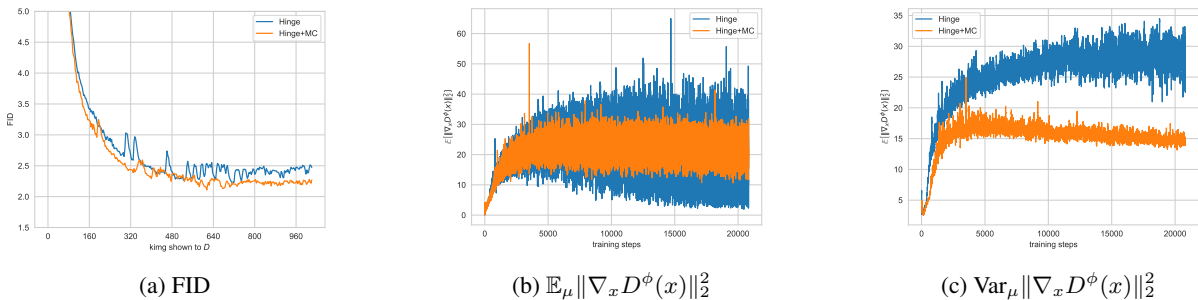


Figure 7: The trend of (a) Fréchet Inception Distance; (b) $\mathbb{E}\|\nabla_x D^\phi(x)\|_2^2$; (c) $\text{Var}\|\nabla_x D^\phi(x)\|_2^2$ for models trained by different methods using CIAFR10 dataset. Here *Hinge* stands for the model trained by Hinge loss, and *Hinge+MC* for the model trained by Hinge loss and our proposed MC method. Lower $\text{Var}_\mu \|\nabla_x D^\phi(x)\|_2^2$ indicate better stability.

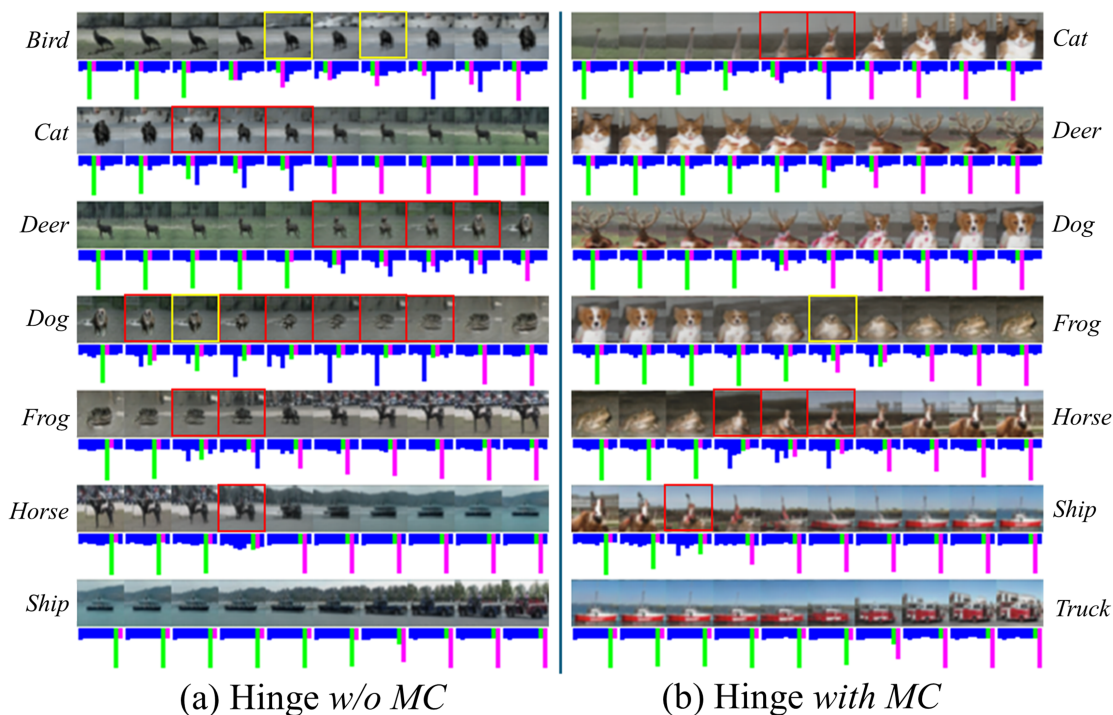


Figure 8: Latent space interpolation based on cStyleGAN2 backbone trained via Hinge loss w/o and with our MC method. Red and yellow boxes highlight two types of undesirable transitions between generated images.

right sides of each row. Each distribution of the confidence scores are calculated by the bottleneck representation of the ResNet-50 classifier with a softened softmax function of temperature 5.0 for normalization. The score bars of the left class and the right class are shown in green and magenta, respectively. The red boxes highlight the images being classified as a third class, while the yellow boxes highlight the images having non-monotonic transitions of their confidence scores compared to those of their adjacent images. In other words, images in both red and yellow boxes are undesirable as they imply that the latent space is less continuous and less smooth. By comparing Figure 8a and 8b, we can see that the MC method performs better in the learned latent space and has most of the decision switch between the two classes occur in the middle range of the interpolation.

5.5 Evaluations of image generation on CIFAR-100

For completeness, we show the image generation performance on CIFAR-100 in Table 4. Significant improvements are achieved by using our MC method independently for both baseline discriminative losses, with average improvement of 1.1 in IS, 1.6 in FID and 3.7 in IFID.

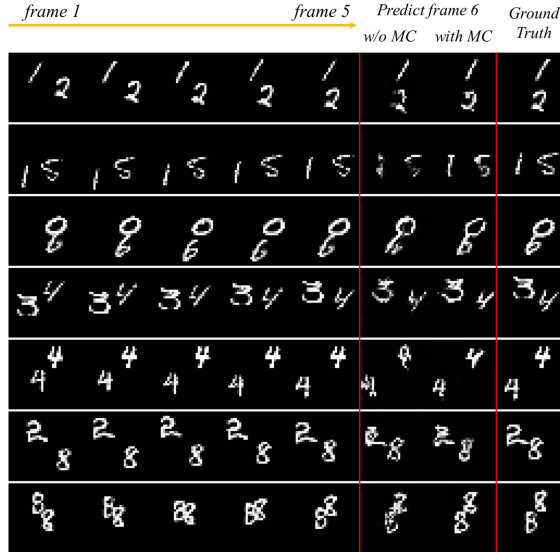


Figure 9: Results of predicting future frame given the past 5 frames based on ConvLSTM w/o and with our MC method.

5.6 Extension to conditional time-series generation

Our MCGAN framework is so flexible that can be incorporated into the conditional time-series generation task, in which case, our goal is to generate future paths based on the past path of the time series. To benchmark with MCGAN, we choose three representative generative models for the time-series generation, i.e. (1) TimeGAN [15]; (2) RCGAN [39] - a conditional GAN; and (3) GMMN [40] - an unconditional maximum mean discrepancy (MMD) with a Gaussian kernel. We trained these models on both vector auto-regressive (VAR) data and stock (S&P 500 and DJI) data. The model performance is evaluated using metrics in [41] including (1) ABS metric - a histogram-based metrics that measure the distance between two distributions; (2) ACF metric - a metric that measures the difference in temporal dependency; (3) R^2 relative error - a metric that demonstrates the effectiveness of synthetic data to be used for real applications. The numerical results illustrate that our MC method can considerably outperform these benchmarks. To be specific, in SPX data, the ABS metric and ACF metric of RCGAN can be improved from 0.01134 to 0.00915 and from 0.03665 to 0.04192 by using our proposed MC method. In VAR dataset, MCGAN also dominates in terms of almost all test metrics under different parameter settings of VAR data.

5.7 Extension to conditional video generation

Inspired by the effectiveness of MCGAN in generation tasks on both spatial image data and temporal time-series data, we also validate our MCGAN model in conditional video generation task. In this task, the generator aims to generate future video frame given the past frames. Here we used Moving MNIST data set [42], which consists of 10,000 20-frame 64x64 videos of moving digits. The whole dataset is divided into the training set (9,000 samples) and the test set (1,000 samples). For the architecture of both generator and discriminator, we use convolutional LSTM (ConvLSTM) unit proposed by [43] due to its effectiveness in video prediction task. In the model training, the generator takes in 5 past frames as the input and generates the corresponding 1-step future frame, then the real past frames and the generated future frames are concatenated along time dimension and put into the discriminator. For comparison, we used classical GAN, which uses BCE as the generative loss, as the benchmark. We trained our model for 10,000 epochs with batch size 16. The model performance is evaluated by computing the MSE between the generated frames and the corresponding ground truth on the test set. From the numerical results, we find that, by using our proposed MC method, the MSE can be improved from 0.153 (GAN) to 0.123 (MCGAN). Compared to the baseline, the predicted frames from our MC method are clearer and more coherent, and visually closer to the ground truth as shown in Figure 9.

6 Conclusion

This paper presents a general MCGAN method to tackle the training instability, a key bottleneck of GANs. Our method enhances generator training by introducing a novel regression loss for (conditional) generative adversarial networks. We establish the optimality and discriminativity of MCGAN, and prove that the convergence of optimal generator can be

achieved under a weaker condition of the discriminator due to the strong supervision of the regression loss. Moreover, extensive numerical results on image data such as Cifar 10 and 100, time series data, and video data are provided to validate the effectiveness and flexibility of our proposed MC-GAN and consistent improvements over the benchmarking GAN models.

For future work, we plan to explore the potential of the MCGAN on larger datasets for high-resolution image generation. We also plan to investigate the effectiveness of the MCGAN in more complex and challenging generation tasks, such as text-to-image generation and image-to-image translation. Last but not least, given the flexibility of the MCGAN on different types of data, we consider generation tasks on data with multiple modalities at the same time.

References

- [1] Ian Goodfellow, Jean Pouget-Abadie, Mehdi Mirza, Bing Xu, David Warde-Farley, Sherjil Ozair, Aaron Courville, and Yoshua Bengio. Generative adversarial nets. *Advances in neural information processing systems*, 27, 2014.
- [2] Ishaan Gulrajani, Faruk Ahmed, Martin Arjovsky, Vincent Dumoulin, and Aaron C Courville. Improved training of wasserstein gans. *Advances in neural information processing systems*, 30, 2017.
- [3] Lars Mescheder, Andreas Geiger, and Sebastian Nowozin. Which training methods for gans do actually converge? In *International conference on machine learning*, pages 3481–3490. PMLR, 2018.
- [4] Takeru Miyato, Toshiki Kataoka, Masanori Koyama, and Yuichi Yoshida. Spectral normalization for generative adversarial networks. *arXiv preprint arXiv:1802.05957*, 2018.
- [5] Minguk Kang, Joonghyuk Shin, and Jaesik Park. Studiogan: A taxonomy and benchmark of gans for image synthesis. *arXiv preprint arXiv:2206.09479*, 2022.
- [6] Martin Arjovsky and Léon Bottou. Towards principled methods for training generative adversarial networks. *arXiv preprint arXiv:1701.04862*, 2017.
- [7] Jae Hyun Lim and Jong Chul Ye. Geometric gan. *arXiv preprint arXiv:1705.02894*, 2017.
- [8] Xudong Mao, Qing Li, Haoran Xie, Raymond YK Lau, Zhen Wang, and Stephen Paul Smolley. Least squares generative adversarial networks. In *Proceedings of the IEEE international conference on computer vision*, pages 2794–2802, 2017.
- [9] Martin Arjovsky, Soumith Chintala, and Léon Bottou. Wasserstein generative adversarial networks. In *International conference on machine learning*, pages 214–223. PMLR, 2017.
- [10] Mehdi Mirza and Simon Osindero. Conditional generative adversarial nets. *arXiv preprint arXiv:1411.1784*, 2014.
- [11] Peng Zhou, Lingxi Xie, Bingbing Ni, Cong Geng, and Qi Tian. Omni-gan: On the secrets of cgans and beyond. In *Proceedings of the IEEE/CVF International Conference on Computer Vision*, pages 14061–14071, 2021.
- [12] Augustus Odena, Christopher Olah, and Jonathon Shlens. Conditional image synthesis with auxiliary classifier gans. In *International conference on machine learning*, pages 2642–2651. PMLR, 2017.
- [13] Minguk Kang, Woohyeon Shim, Minsu Cho, and Jaesik Park. Rebooting acgan: Auxiliary classifier gans with stable training. *Advances in Neural Information Processing Systems*, 34:23505–23518, 2021.
- [14] Changhee Han, Hideaki Hayashi, Leonardo Rundo, Ryosuke Araki, Wataru Shimoda, Shinichi Muramatsu, Yujiro Furukawa, Giancarlo Mauri, and Hideki Nakayama. Gan-based synthetic brain mr image generation. In *2018 IEEE 15th international symposium on biomedical imaging (ISBI 2018)*, pages 734–738. IEEE, 2018.
- [15] Jinsung Yoon, Daniel Jarrett, and Mihaela Van der Schaar. Time-series generative adversarial networks. *Advances in neural information processing systems*, 32, 2019.
- [16] Tianlin Xu, Li Kevin Wenliang, Michael Munn, and Beatrice Acciaio. Cot-gan: Generating sequential data via causal optimal transport. *Advances in neural information processing systems*, 33:8798–8809, 2020.
- [17] Hao Ni, Lukasz Szpruch, Marc Sabate-Vidales, Baoren Xiao, Magnus Wiese, and Shujian Liao. Sig-wasserstein gans for time series generation. In *Proceedings of the Second ACM International Conference on AI in Finance*, pages 1–8, 2021.
- [18] Sonam Gupta, Arti Keshari, and Sukhendu Das. Rv-gan: Recurrent gan for unconditional video generation. In *Proceedings of the IEEE/CVF Conference on Computer Vision and Pattern Recognition*, pages 2024–2033, 2022.
- [19] Shujian Liao, Hao Ni, Marc Sabate-Vidales, Lukasz Szpruch, Magnus Wiese, and Baoren Xiao. Sig-wasserstein gans for conditional time series generation. *Mathematical Finance*, 34(2):622–670, 2024.

- [20] Lei Xu, Maria Skoularidou, Alfredo Cuesta-Infante, and Kalyan Veeramachaneni. Modeling tabular data using conditional gan. *Advances in neural information processing systems*, 32, 2019.
- [21] Takeru Miyato and Masanori Koyama. cgans with projection discriminator. *arXiv preprint arXiv:1802.05637*, 2018.
- [22] Liang Hou, Qi Cao, Huawei Shen, Siyuan Pan, Xiaoshuang Li, and Xueqi Cheng. Conditional gans with auxiliary discriminative classifier. In *International Conference on Machine Learning*, pages 8888–8902. PMLR, 2022.
- [23] Junbo Zhao, Michael Mathieu, and Yann LeCun. Energy-based generative adversarial network. *arXiv preprint arXiv:1609.03126*, 2016.
- [24] Shuang Liu, Olivier Bousquet, and Kamalika Chaudhuri. Approximation and convergence properties of generative adversarial learning. *Advances in Neural Information Processing Systems*, 30, 2017.
- [25] Tim Salimans, Ian Goodfellow, Wojciech Zaremba, Vicki Cheung, Alec Radford, and Xi Chen. Improved techniques for training gans. *Advances in neural information processing systems*, 29, 2016.
- [26] Krizhevsky Alex. Learning multiple layers of features from tiny images. <https://www.cs.toronto.edu/kriz/learning-features-2009-TR.pdf>, 2009.
- [27] Andrew Brock, Jeff Donahue, and Karen Simonyan. Large scale gan training for high fidelity natural image synthesis. *arXiv preprint arXiv:1809.11096*, 2018.
- [28] Tero Karras, Samuli Laine, Miika Aittala, Janne Hellsten, Jaakko Lehtinen, and Timo Aila. Analyzing and improving the image quality of stylegan. In *Proceedings of the IEEE/CVF conference on computer vision and pattern recognition*, pages 8110–8119, 2020.
- [29] Tero Karras, Timo Aila, Samuli Laine, and Jaakko Lehtinen. Progressive growing of gans for improved quality, stability, and variation. *arXiv preprint arXiv:1710.10196*, 2017.
- [30] Shengyu Zhao, Zhijian Liu, Ji Lin, Jun-Yan Zhu, and Song Han. Differentiable augmentation for data-efficient gan training. *Advances in Neural Information Processing Systems*, 33:7559–7570, 2020.
- [31] Andrew L Maas, Awni Y Hannun, Andrew Y Ng, et al. Rectifier nonlinearities improve neural network acoustic models. In *Proc. icml*, volume 30, page 3. Atlanta, GA, 2013.
- [32] Tero Karras, Miika Aittala, Janne Hellsten, Samuli Laine, Jaakko Lehtinen, and Timo Aila. Training generative adversarial networks with limited data. *Advances in Neural Information Processing Systems*, 33:12104–12114, 2020.
- [33] Han Zhang, Zizhao Zhang, Augustus Odena, and Honglak Lee. Consistency regularization for generative adversarial networks. *arXiv preprint arXiv:1910.12027*, 2019.
- [34] Shane Barratt and Rishi Sharma. A note on the inception score. *arXiv preprint arXiv:1801.01973*, 2018.
- [35] Martin Heusel, Hubert Ramsauer, Thomas Unterthiner, Bernhard Nessler, and Sepp Hochreiter. Gans trained by a two time-scale update rule converge to a local nash equilibrium. *Advances in neural information processing systems*, 30, 2017.
- [36] Terrance DeVries, Adriana Romero, Luis Pineda, Graham W Taylor, and Michal Drozdal. On the evaluation of conditional gans. *arXiv preprint arXiv:1907.08175*, 2019.
- [37] Kaiming He, Xiangyu Zhang, Shaoqing Ren, and Jian Sun. Deep residual learning for image recognition. In *Proceedings of the IEEE conference on computer vision and pattern recognition*, pages 770–778, 2016.
- [38] Hung-Yu Tseng, Lu Jiang, Ce Liu, Ming-Hsuan Yang, and Weilong Yang. Regularizing generative adversarial networks under limited data. In *Proceedings of the IEEE/CVF Conference on Computer Vision and Pattern Recognition*, pages 7921–7931, 2021.
- [39] Cristóbal Esteban, Stephanie L Hyland, and Gunnar Rätsch. Real-valued (medical) time series generation with recurrent conditional gans. *arXiv preprint arXiv:1706.02633*, 2017.
- [40] Yujia Li, Kevin Swersky, and Rich Zemel. Generative moment matching networks. In *International conference on machine learning*, pages 1718–1727. PMLR, 2015.
- [41] Shujian Liao, Hao Ni, Lukasz Szpruch, Magnus Wiese, Marc Sabate-Vidales, and Baoren Xiao. Conditional sig-wasserstein gans for time series generation. *arXiv preprint arXiv:2006.05421*, 2020.
- [42] Nitish Srivastava, Elman Mansimov, and Ruslan Salakhudinov. Unsupervised learning of video representations using lstms. In *International conference on machine learning*, pages 843–852. PMLR, 2015.
- [43] Xingjian Shi, Zhoung Chen, Hao Wang, Dit-Yan Yeung, Wai-Kin Wong, and Wang-chun Woo. Convolutional lstm network: A machine learning approach for precipitation nowcasting. *Advances in neural information processing systems*, 28, 2015.

- [44] Sebastian Nowozin, Botond Cseke, and Ryota Tomioka. f-gan: Training generative neural samplers using variational divergence minimization. *Advances in neural information processing systems*, 29, 2016.
- [45] XuanLong Nguyen, Martin J Wainwright, and Michael I Jordan. Estimating divergence functionals and the likelihood ratio by convex risk minimization. *IEEE Transactions on Information Theory*, 56(11):5847–5861, 2010.
- [46] Nitish Shirish Keskar, Dheevatsa Mudigere, Jorge Nocedal, Mikhail Smelyanskiy, and Ping Tak Peter Tang. On large-batch training for deep learning: Generalization gap and sharp minima. *arXiv preprint arXiv:1609.04836*, 2016.

A Proofs

A.1 Proof of optimality

Proof For every $\phi \in \Phi$, the derivative of $L_G(\theta; \phi, \mu)$ in (5) w.r.t θ can be derived as

$$\begin{aligned}\nabla_{\theta} L_G(\theta; \phi, \mu) &= \mathbb{E}_{\mu}[2(D^{\phi}(x) - \mathbb{E}_{\nu_{\theta}}[D^{\phi}(x)])H(\theta, \phi)], \\ &= 2(\mathbb{E}_{\nu_{\theta}}[D^{\phi}(x)] - \mathbb{E}_{\mu}[D^{\phi}(x)])H(\theta, \phi),\end{aligned}$$

where

$$H(\theta, \phi) = \mathbb{E}_{z \sim p(z)}[(\nabla_{\theta} G^{\theta}(z))^T \cdot \nabla_x D^{\phi}(G^{\theta}(z))].$$

If θ^* is a local minimizer of $L_G(\theta; \phi, \mu)$, then by first-order condition, it satisfies that

$$\mathbb{E}_{\nu_{\theta^*}}[D^{\phi}(x)] - \mathbb{E}_{\mu}[D^{\phi}(x)] = 0, \quad (20)$$

or

$$H(\theta^*, \phi) = \vec{0}. \quad (21)$$

By Assumption 3.1, equation (21) holds only if $\nu_{\theta^*} = \mu$. Here we focus on the other case (20).

Given a parameterization map $\phi'_{\cdot, \cdot} : \mathcal{P}(\mathcal{X}) \times \mathcal{P}(\mathcal{X}) \rightarrow \Phi$ and $D^{\phi'_{\cdot, \cdot}} \in \mathcal{D}_{\text{Dis}}$, if θ^* is a local minimizer of $L_G(\theta; \phi'_{\mu, \nu_{\theta^*}}, \mu)$, we must have

$$\mathbb{E}_{\nu_{\theta^*}}[D^{\phi'_{\mu, \nu_{\theta^*}}}(x)] - \mathbb{E}_{\mu}[D^{\phi'_{\mu, \nu_{\theta^*}}}(x)] = 0. \quad (22)$$

Since $D^{\phi'_{\cdot, \cdot}} \in \mathcal{D}_{\text{Dis}}$, without generality, we set $a = 1$ and $c = 0$ and have

$$\begin{aligned}&\mathbb{E}_{\nu_{\theta}}[D^{\phi'_{\mu, \nu_{\theta}}}(x)] - \mathbb{E}_{\mu}[D^{\phi'_{\mu, \nu_{\theta}}}(x)] \\ &= \int_{\mathcal{A}^{\mu, \nu_{\theta}}} D^{\phi'_{\mu, \nu_{\theta}}}(x)(p_{\mu}(x) - p_{\nu_{\theta}}(x))dx \\ &> 0,\end{aligned} \quad (23)$$

for every different μ and ν_{θ} . Hence equality (22) holds if and only if $\nu_{\theta^*} = \mu$, which completes the proof. \blacksquare

A.2 Proof of f -divergence

Lemma 4.1 *Given the optimal discriminator in (13), optimizing the MCGAN objective (5) is equivalent to minimizing the square of f -divergence:*

$$\nabla_{\theta} \mathcal{L}_G(\theta; \phi^*) = \nabla_{\theta} [\text{Div}_f(\mu \|\bar{\nu})]^2, \quad (15)$$

where $f(x) = x(x-1)$.

Proof Given the optimal discriminator in (13), we have

$$\begin{aligned}&\mathbb{E}_{\mu}[D^{\phi^*}(x)] - \mathbb{E}_{\nu_{\theta}}[D^{\phi^*}(x)] \\ &= \int_{\text{supp } \mu \cup \text{supp } \nu_{\theta}} \frac{p_{\mu}(x)}{p_{\mu}(x) + p_{\nu_{\theta}}(x)} (p_{\mu}(x) - p_{\nu_{\theta}}(x)) dx.\end{aligned}$$

Let $\bar{\nu} := \frac{\mu + \nu_{\theta}}{2}$ be the averaged measure defined on $\text{supp } \mu \cup \text{supp } \nu_{\theta}$, then we have

$$\begin{aligned}&\mathbb{E}_{\mu}[D^{\phi^*}(x)] - \mathbb{E}_{\nu_{\theta}}[D^{\phi^*}(x)] \\ &= \int_{\text{supp } \mu \cup \text{supp } \nu_{\theta}} \frac{p_{\mu}(x)}{2p_{\bar{\nu}}(x)} \frac{(p_{\mu}(x) - p_{\nu_{\theta}}(x))}{p_{\bar{\nu}}(x)} p_{\bar{\nu}}(x) dx \\ &= \int_{\text{supp } \mu \cup \text{supp } \nu_{\theta}} \frac{p_{\mu}(x)}{p_{\bar{\nu}}(x)} \left(\frac{p_{\mu}(x)}{p_{\bar{\nu}}(x)} - 1 \right) p_{\bar{\nu}}(x) dx \\ &= \int_{\text{supp } \mu \cup \text{supp } \nu_{\theta}} f\left(\frac{p_{\mu}(x)}{p_{\bar{\nu}}(x)}\right) p_{\bar{\nu}}(x) dx \\ &= \text{Div}_f(\mu \|\bar{\nu}),\end{aligned}$$

where $f(x) := x(x - 1)$ is a convex function and $f(1) = 0$. Therefore, $\text{Div}_f(\mu \parallel \bar{\nu})$ is well-defined f -divergence. Furthermore, we can observe that the gradient of the generator objective function $L_G(\theta; \phi^*)$ can be written as the gradient of the squared f -divergence:

$$\begin{aligned}\nabla_{\theta} L_G(\theta; \phi^*) &= \nabla_{\theta} \mathbb{E}_{\mu} \left[D^{\phi^*}(x) - \mathbb{E}_{\nu_{\theta}}[D^{\phi^*}(x)] \right]^2 \\ &= \nabla_{\theta} \left[\mathbb{E}_{\mu}[D^{\phi^*}(x)] - \mathbb{E}_{\nu_{\theta}}[D^{\phi^*}(x)] \right]^2 \\ &= \nabla_{\theta} [\text{Div}_f(\mu \parallel \bar{\nu})]^2,\end{aligned}$$

which completes the proof. ■

A.3 Proof of improved stability

Theorem 4.1 *Let $D^{\phi_{\epsilon}}(x)$ be a noisy version of optimal discriminator such that $D^{\phi_{\epsilon}}(x) = D^{\phi^*}(x) + \epsilon_1(x)$ and $\nabla_x D^{\phi_{\epsilon}}(x) = \nabla_x D^{\phi^*}(x) + \epsilon_2(x)$ for $\forall x \in \mathcal{X}$, where $\epsilon_1(x)$ and $\epsilon_2(x)$ are two uncorrelated and centred random noises that are indexed by x and have finite variance.⁶ Then for $\mathcal{L}_G(\theta; \phi)$ in (5), we have*

$$\mathbb{E}[\nabla_{\theta} \mathcal{L}_G(\theta; \phi_{\epsilon})] = \nabla_{\theta} \mathcal{L}_G(\theta; \phi^*), \quad (16)$$

and the variance of $\nabla_{\theta} \mathcal{L}_G(\theta; \phi_{\epsilon})$ is finite and depends on the difference between μ and ν_{θ} . Specifically, when $\nu_{\theta^*} = \mu$, we have $\nabla_{\theta} \mathcal{L}_G(\theta^*; \phi_{\epsilon}) = 0$ almost surely.

Proof Since $D^{\phi_{\epsilon}}(x) = D^{\phi^*}(x) + \epsilon_1(x)$ and $\nabla_x D^{\phi_{\epsilon}}(x) = \nabla_x D^{\phi^*}(x) + \epsilon_2(x)$, we have

$$\begin{aligned}\nabla_{\theta} L_G(\theta; \phi_{\epsilon}) &= \left(\mathbb{E}_{\nu_{\theta}}[D^{\phi_{\epsilon}}(x)] - \mathbb{E}_{\mu}[D^{\phi_{\epsilon}}(x)] \right) H(\theta, \phi_{\epsilon}) \\ &= \left(\mathbb{E}_{\nu_{\theta}}[D^{\phi^*}(x)] - \mathbb{E}_{\mu}[D^{\phi^*}(x)] + \mathbb{E}_{\nu_{\theta}}[\epsilon_1(x)] - \mathbb{E}_{\mu}[\epsilon_1(x)] \right) H(\theta, \phi_{\epsilon}) \\ &= (\Delta(\theta, \phi^*) + \bar{\epsilon}_1(\theta)) H(\theta, \phi_{\epsilon}),\end{aligned}$$

where

$$\Delta(\theta, \phi) = \mathbb{E}_{\nu_{\theta}}[D^{\phi}(x)] - \mathbb{E}_{\mu}[D^{\phi}(x)]$$

and

$$\bar{\epsilon}_1(\theta) = \mathbb{E}_{\nu_{\theta}}[\epsilon_1(x)] - \mathbb{E}_{\mu}[\epsilon_1(x)].$$

Because

$$\begin{aligned}H(\theta, \phi_{\epsilon}) &= \mathbb{E}_{z \sim \mu_z} [(\nabla_{\theta} G^{\theta}(z))^T \cdot \nabla_x D^{\phi_{\epsilon}}(G^{\theta}(z))] \\ &= H(\theta, \phi^*) + \mathbb{E}_{z \sim \mu_z} [(\nabla_{\theta} G^{\theta}(z))^T \cdot \epsilon_2(x)] \\ &= H(\theta, \phi^*) + \bar{\epsilon}_2(\theta),\end{aligned}$$

we have

$$\begin{aligned}\nabla_{\theta} L_G(\theta; \phi_{\epsilon}) &= \Delta(\theta, \phi^*) H(\theta, \phi^*) + \bar{\epsilon}_1(\theta) H(\theta, \phi^*) + \Delta(\theta, \phi^*) \bar{\epsilon}_2(\theta) + \bar{\epsilon}_1(\theta) \bar{\epsilon}_2(\theta) \\ &= \nabla_{\theta} L_G(\theta; \phi^*) + \bar{\epsilon}_1(\theta) H(\theta, \phi^*) + \Delta(\theta, \phi^*) \bar{\epsilon}_2(\theta) + \bar{\epsilon}_1(\theta) \bar{\epsilon}_2(\theta).\end{aligned}$$

Since both $\bar{\epsilon}_1(\theta)$ and $\bar{\epsilon}_2(\theta)$ are weighted averages or linear combinations of centred random noises, they are both centred noises as well. Moreover, the expectation of $\bar{\epsilon}_1(\theta) \bar{\epsilon}_2(\theta)$ is also zero since $\epsilon_1(x)$ and $\epsilon_2(x)$ are uncorrelated. Hence the mean of $\nabla_{\theta} L_G(\theta; \phi_{\epsilon})$ equals to $\nabla_{\theta} L_G(\theta; \phi^*)$. By the definition of $\Delta(\theta, \phi)$ and $\bar{\epsilon}_1(\theta)$, its variance also depends on the difference between μ and ν_{θ} , which completes the proof. ■

A.4 Discriminability

Here we provide the of the discriminability of optimal discriminators in these GAN variants described in Table 1.

⁶This assumption of centred random noise is made due to the fact that as the approximation gets better, this error looks more and more like centred random noise due to the finite precision [6].

- **Vanilla GAN [1]:** GAN employs BCE as the discriminative loss function defined as

$$L_D(\phi; \mu, \nu_\theta) = \mathbb{E}_\mu [\log(D^\phi(X))] + \mathbb{E}_{\nu_\theta} [\log(1 - D^\phi(X))]. \quad (24)$$

As proven in [1], the optimal discriminator given binary cross-entropy loss can be derived as:

$$D^{\phi^*, \nu_\theta}(x) = \frac{p_\mu(x)}{p_\mu(x) + p_{\nu_\theta}(x)}. \quad (25)$$

Let us consider function $f(l) = \frac{1}{1+l}$ for $l > 0$. Notice that $f(l) > 1/2$ when $l < 1$, and $f(l) < 1/2$ when $l > 1$. Also notice that $D^{\phi^*, \nu_\theta}(x) = f(\frac{p_{\nu_\theta}(x)}{p_\mu(x)})$, it is easy to verify that $(D^{\phi^*, \nu_\theta}(x) - 1/2)(p_\mu(x) - p_{\nu_\theta}(x)) > 0$ when $p_\mu(x) \neq p_{\nu_\theta}(x)$.

- **Least Square GAN [8]:** LSGAN employs least square loss function defined as follows:

$$L_D(\phi; \mu, \nu_\theta) = -\mathbb{E}_\mu [(D^\phi(X) - \alpha)^2] - \mathbb{E}_{\nu_\theta} [(D^\phi(X) - \beta)^2],$$

where $\alpha, \beta \in \mathbb{R}$, and $\alpha \neq \beta$. The optimal discriminator is given as

$$D^{\phi^*, \nu_\theta}(x) = \frac{\alpha p_\mu(x) + \beta p_{\nu_\theta}(x)}{p_\mu(x) + p_{\nu_\theta}(x)}, \quad (26)$$

Similarly, by the fact that $D^{\phi^*}(x) = f(\frac{p_{\nu_\theta}(x)}{p_\mu(x)})$, where $f(l) = \frac{\alpha + \beta l}{1+l}$, we can verify that this discriminator also has (strict) discriminability in the sense that $\text{sign}(\alpha - \beta)(D^{\phi^*, \nu_\theta}(x) - \frac{\alpha + \beta}{2})(p_\mu(x) - p_{\nu_\theta}(x)) > 0$ when $p_\mu(x) \neq p_{\nu_\theta}(x)$.

- **Geometric GAN [7]:** Hinge loss function is defined as

$$L_D(\phi; \mu, \nu_\theta) = -\mathbb{E}_\mu [\max(0, 1 - D^\phi(X))] - \mathbb{E}_{\nu_\theta} [\max(0, 1 + D^\phi(X))].$$

By Lemma B.1 in [7], it is straightforward to show that the optimal discriminator can be derived as:

$$D^{\phi^*, \nu_\theta}(x) = 2\mathbb{1}_{\{p_\mu(x) \geq p_{\nu_\theta}(x)\}} - 1. \quad (27)$$

It is clear that $D^{\phi^*}(x) = f(\frac{p_\mu(x)}{p_{\nu_\theta}(x)})$, where $f(l) = 2\mathbb{1}_{\{l \geq 1\}} - 1$, and $D^{\phi^*}(x)(p_\mu(x) - p_{\nu_\theta}(x)) > 0$ when $p_\mu(x) \neq p_{\nu_\theta}(x)$.

- **Energy-based GAN [23]:** Energy-based loss function is defined as

$$L_D(\phi; \mu, \nu_\theta) = -\mathbb{E}_\mu [D^\phi(X)] - \mathbb{E}_{\nu_\theta} [\max(0, m - D^\phi(X))].$$

where $m > 0$. By Lemma 1 in [23], the optimal discriminator given energy-based loss function can be derived as:

$$D^{\phi^*, \nu_\theta}(x) = m\mathbb{1}_{\{p_\mu(x) < p_{\nu_\theta}(x)\}}. \quad (28)$$

It is straight forward to verify that $-m(D^{\phi^*, \nu_\theta}(x) - m/2)(p_\mu(x) - p_{\nu_\theta}(x)) > 0$ when $p_\mu(x) \neq p_{\nu_\theta}(x)$.

- **f -GAN [44]:** In f -GAN, variational lower bound (VLB) on the f -divergence $\text{Div}_f(\mu || \nu_\theta)$ is used in the generative-adversarial approach to mimic the target distribution ν_θ . Let $f : \mathbb{R}_+ \rightarrow \mathbb{R}$ be a convex, lower-semicontinuous function. In f -GAN, the discriminative loss is defined as the variational lower bound on certain f -divergence:

$$L_D(\phi; \mu, \nu_\theta) = \mathbb{E}_\mu [D^\phi(X)] - \mathbb{E}_{\nu_\theta} [f^*(D^\phi(X))], \quad (29)$$

where f^* is the convex conjugate function of f . Under mild conditions on function f [45], the maximum of (29) is achieved when

$$D^{\phi^*, \nu_\theta}(x) = f' \left(\frac{p_\mu(x)}{p_{\nu_\theta}(x)} \right), \quad (30)$$

where f' is the first order derivative of f and increasing due to the convexity of f . Consequently, we can choose $c = f'(1)$ such that $(D^{\phi^*, \nu_\theta}(x) - c)(p_\mu(x) - p_{\nu_\theta}(x)) > 0$ when $p_\mu(x) \neq p_{\nu_\theta}(x)$. A more detailed list of f -divergence can be found in [44].

B Architectures, hyperparameters, and training techniques

B.1 BigGAN architecture

Table 5 shows the architectural details.

$z \in \mathbb{R}^{128} \sim \mathcal{N}(0, I)$	RGB image $x \in \mathbb{R}^{32 \times 32 \times 3}$
SNLinear 128 $\rightarrow 4 \times 4 \times 4ch$	DResBlock down 3 $\rightarrow 4ch$
GResBlock up $4ch \rightarrow 4ch$	DResBlock down $4ch \rightarrow 4ch$
GResBlock up $4ch \rightarrow 4ch$	DResBlock down $4ch \rightarrow 4ch$
GResBlock up $4ch \rightarrow 4ch$	DResBlock down $4ch \rightarrow 4ch$
BN, ReLU, 3×3 SNConv $4ch \rightarrow 3$	SumPooling
Activation: Tanh	SNLinear $4ch \rightarrow 1$, embed(y) $\in \mathbb{R}^{256}$
(a) Generator	(b) Discriminator

Table 5: BigGAN architecture used in CIFAR-10 and CIFAR-100 experiment, where ch is set as 64.

B.2 Choice of MC size

In the BigGAN experiment, the MC size we used is 10. While in the StyleGAN experiment, the MC size is only 4. While the MC size we choose is surprisingly small, MCGAN still achieves superior performance on conditional image generation tasks. It might be counter-intuitive that a large MC size will not necessarily result in a better generator. Although a larger MC size will lead to more accurate estimated conditions, it might deteriorate the generalization of the generator network. As explored in [46], large batch size usually leads to a loss in generalization performance. While the small batch method achieves low precision, it tends to have better performance on the test set than the large batch size which is very similar to the bias-variance trade-off. For the same reason, we would not choose a large MC size which will not necessarily lead to better performance, not to mention the enormously increased computational cost it can raise.

B.3 Weight decay

To prevent overfitting of the discriminator, we apply weight decay. It is observed that a high weight decay value can deteriorate the model performance, hence we need to choose the weight decay value carefully. We also found empirically that the value of weight decay is often related to the diversity of the training set. Hence the weight decay we suggest for the discriminator is 0.001 in the CIFAR-10 experiment and 0.005 for the CIFAR-100 experiment, as we have a very limited training sample per class in the CIFAR-100 dataset. When combining weight decay with differentiable augmentation, we chose a low level of weight decay for the discriminator, that is 0.0001 as the differentiable augmentation also improved the diversity of training samples.

As recommended in [11], we also applied weight decay to the generator as it was found that the generator can also have an overfitting problem and that applying weight decay on the generator makes the training more stable. That is probably due to the fact that at the late stage of training, the generator focus on generating images that achieves high logits, which harms the diversity of generated samples. Hence we also set the weight decay of the generator as 0.0001 to avoid the risk of overfitting.

C Algorithm

The algorithm for the conditional generation task can be found in Algorithm 1.

ALGORITHM 1: Algorithm of MCGAN

Input:

- N : the number of epochs;
- N_D : number of discriminator iterations per generator iteration;
- $B \in \mathbb{N}$: batch size;
- N_{MC} : the number of Monte Carlo samples;
- f : specified function used to compute discriminative loss.
- $C_{(lb,ub)}$: the clamp function with lower bound lb and upper bound ub .

Output:

(θ^*, ψ^*) : approximation of the optimal parameters of the generator and discriminator.

1: Initialize the model parameter (θ, ψ) of the generator G and discriminator D . **for** $n = 1 : N$ **do**

for $n_d = 1 : N_D$ **do**

2: Sample batch $\{(x_i, y_i)\}_{i=1}^B \sim p_d(X, Y)$

3: Generate fake samples given labels $\{(\hat{x}_i, y_i)\}_{i=1}^B \sim p_\theta(X, Y)$

4: Compute discriminative loss:

$$\mathcal{L}_D(\phi; \mu, \nu_\theta) \leftarrow \frac{1}{B} \sum_{i=1}^B f_1(D^\psi(x_i, y_i)) + \frac{1}{B} \sum_{i=1}^B f_2(D^\psi(\hat{x}_i, y_i));$$

5: Update parameter of discriminator:

$$\psi \leftarrow \text{Adam}(\mathcal{L}_D)$$

end

6: Sample batch $\{(x_i, y_i)\}_{i=1}^B \sim p_d(X, Y)$

7: For each label y_i , estimate the conditional expectation

$$\begin{aligned} \hat{\mathbb{E}}_{p_\theta}[C_{(lb,ub)}(D^\psi(X, y_i))|y_i] \leftarrow \\ \frac{1}{N_{mc}} \sum_{j=1}^{N_{mc}} C_{(lb,ub)}(D^\psi(G^\theta(y_i, z^{(j)}), y_i)) \end{aligned}$$

8: Compute generative loss:

$$\mathcal{L}_G \leftarrow$$

$$\frac{1}{B} \sum_{i=1}^B \|C_{(lb,ub)}D^\psi(x_i, y_i) - \hat{\mathbb{E}}_{p_\theta}[C_{(lb,ub)}(D^\psi(X, y_i))|y_i]\|^2;$$

9: Update parameter of generator:

$$\theta \leftarrow \text{Adam}(\mathcal{L}_G)$$

end
